

Magnetization plateau in a two-dimensional multiple-spin exchange model

Tsutomu Momoi, Harumi Sakamoto and Kenn Kubo
Institute of Physics, University of Tsukuba, Tsukuba, Ibaraki 305-8571, Japan
(February 5, 2020)

We study a multiple-spin exchange model on a triangular lattice, which is a possible model for low-density solid ^3He films. Due to strong competitions between ferromagnetic three-spin exchange and antiferromagnetic four-spin one, the ground states are highly degenerate in the classical limit. At least $2^{L/2}$ -fold degeneracy exists on the $L \times L$ triangular lattice except for the $SO(3)$ symmetry. In the magnetization process, we found a plateau at $m/m_{\text{sat}} = 1/2$, in which the ground state is $uuud$ state (a collinear state with four sublattices). The $1/2$ -plateau appears due to the strong four-spin exchange interaction. This plateau survives against both quantum and thermal fluctuations. Under a magnetic field which realizes the $uuud$ ordered state, a phase transition occurs at a finite temperature. We predict that low-density solid ^3He thin films may show the $1/2$ -plateau in the magnetization process. Experimental observation of the plateau will verify strength of the four-spin exchange.

PACS numbers: 67.80.Jd, 75.60.-d, 67.70.+n, 75.40.Cx

I. INTRODUCTION

In localized fermion systems, the magnetic interaction comes from permutations of particles.^{1,2} Multiple-spin exchanges, e.g. cyclic exchanges of three or four spins, have been revealed to be strong in nuclear magnetism of two-dimensional (2D) solid ^3He films. Many experimental^{3–5} and theoretical^{6–10} studies suggested that exchange interactions of more-than-two spins are dominant in this system. A ferromagnetic behavior changes to antiferromagnetic one when the coverage of ^3He decreases.^{11–15} This tendency can be understood in terms of multiple-spin exchange (MSE): in fully packed systems, the three-spin exchange is dominant⁶ and it is ferromagnetic (as shown by Thouless²), and, in loosely packed systems, the four- and six-spin exchanges become strong and favor antiferromagnetism. Effects of multiple-spin exchanges are not yet fully understood especially for the low-density region.^{16,5} For example, recent specific-heat data at low densities show a peculiar behavior, which have a double-peak structure, and they also show that the ground state seems to be spin liquid (disordered) and the spin excitation gap is vanishing (or quite small).⁵

The multiple-spin exchange (MSE) model has been studied to describe the nuclear magnetism of three-dimensional solid ^3He .¹⁷ A general form of the spin Hamiltonian of quantum solid is^{1,2} $\mathcal{H} = -\sum_n (-1)^n J_n \sum_{P_n} P_n$, where P_n and $J_n (\leq 0)$ denote cyclic permutation of n spins and its exchange constant, respectively. For the 2D system, recent theoretical calculations^{8–10} and experimental measurements⁴ found that the exchange frequencies satisfy $|J_3| > |J_2| > |J_4| \gtrsim |J_6| \gtrsim |J_5|$ on the triangular lattice. In this paper, we consider a spin model with the two-, three-, and four-spin exchanges on the triangular lattice, which is the simplest 2D MSE model. Since the three-spin exchange can be transformed to the two-spin ones, the Hamiltonian can

be written with two parameters J and K as

$$\mathcal{H} = J \sum_{\langle i,j \rangle} \boldsymbol{\sigma}_i \cdot \boldsymbol{\sigma}_j + K \sum_p h_p - \mu B \sum_i \sigma_i^z, \quad (1)$$

where $\boldsymbol{\sigma}_i$ denote Pauli matrices. The last term means the Zeeman energy, where μ denotes the nuclear magnetic moment of ^3He and B the magnetic field. The parameter $J (= J_3 - J_2/2)$ is negative for most of densities, (but it can change the sign,) and $K (= -J_4/4)$ is always positive ($K \geq 0$). The first and the second summations run over all pairs of nearest neighbors and all minimum diamond clusters, respectively. The explicit form of h_p for four sites (1, 2, 3, 4) is

$$\begin{aligned} h_p &= 4(P_4 + P_4^{-1}) - 1 \\ &= \sum_{1 \leq i < j \leq 4} \boldsymbol{\sigma}_i \cdot \boldsymbol{\sigma}_j + (\boldsymbol{\sigma}_1 \cdot \boldsymbol{\sigma}_2)(\boldsymbol{\sigma}_3 \cdot \boldsymbol{\sigma}_4) \\ &\quad + (\boldsymbol{\sigma}_1 \cdot \boldsymbol{\sigma}_4)(\boldsymbol{\sigma}_2 \cdot \boldsymbol{\sigma}_3) - (\boldsymbol{\sigma}_1 \cdot \boldsymbol{\sigma}_3)(\boldsymbol{\sigma}_2 \cdot \boldsymbol{\sigma}_4), \end{aligned} \quad (2)$$

where (1, 3) and (2, 4) are diagonal bonds of the diamond. The WKB approximations^{7,9} show that exchange parameters vary depending on the particle density: At high densities, the exchange $J (\leq 0)$ is dominant, which mainly originates from the three spin exchange. As lowering the density, the ratio $|K/J|$ increases rapidly and hence the four spin exchange $K (\geq 0)$ becomes important. This density dependence is consistent with experimental results of susceptibility.^{11–15} Since multiple-spin exchanges produce frustration by themselves and strong competitions between exchanges also introduce frustration,¹⁸ this model is expected to show various complex magnetic behaviors.

In a previous paper, we studied the ground state of this model in the classical limit and found various phases:¹⁹ (a) For $J < -8K$, the ground state shows the perfect ferromagnetism. (b) For $-8K < J < -8K/3$, ground states are highly degenerate. This degeneracy is a non-trivial one. (c) In $-8K/3 < J < 25K/3$, the ground state has a

four-sublattice structure with zero magnetization, which we call as the tetrahedral structure.²⁰ (d) For $25K/3 < J$, the ground state is the so-called 120° structure. Thus novel phases (b) and (c) appear due to the four-spin exchange interactions. In the region (c), we predicted chiral symmetry breaking at a finite temperature.²⁰

The intermediate phase (b) seems to correspond to the parameter region of 2D low-density solid ^3He . The parameters J and K in the low density region are estimated as $J \simeq -6(\text{mK})$ and $K \simeq 1.5(\text{mK})$ from susceptibility and specific-heat data,⁴ and $J/K = -4 \pm 2$ from path integral Monte Carlo simulations^{8–10}. The five- and six-spin exchanges are also estimated to be comparable with four-spin one. This parameter region almost belongs to the phase (b) of our study in the classical limit. Our previous study¹⁹ shows that competitions between the two- and four-spin exchanges are strong in this phase and many kinds of ground states exist due to frustration. Furthermore, we found that under the magnetic field a plateau appears at $m/m_{\text{sat}} = 1/2$ in the magnetization curve, where m_{sat} denotes the saturated magnetization. These various unusual phenomena occur due to frustration caused by the multi-spin exchanges. In this paper we study this phase further, especially considering quantum effects. Finite-temperature effects are also discussed.

In section II we summarize the results for the phase (b) of the classical model. Among degenerate ground states, one collinear state, which we call *uuud* state, has the largest magnetization, $m/m_{\text{sat}} = 1/2$, and other states show $m/m_{\text{sat}} < 1/2$. In section III we discuss the quantum model. Due to quantum effects, the *uuud* state disappears from the ground state and the ground state belongs to the $S = 0$ space. Magnetization process of the quantum model is studied in section IV. Under the magnetic field, the *uuud* ordered state becomes stable, since it has the largest magnetization, and makes a plateau at $m/m_{\text{sat}} = 1/2$ in the magnetization curve. We discuss thermal effects in section V. Under the magnetic field, which realizes the *uuud* ground state, the system shows a finite-temperature phase transition. Section VI contains summaries and discussions.

II. CLASSICAL LIMIT

We studied the ground state of the model (1) in the classical limit,¹⁹ where the Pauli matrices are replaced to unit vectors (u_i^x, u_i^y, u_i^z) with $|u_i^x|^2 + |u_i^y|^2 + |u_i^z|^2 = 1$. We searched the ground state using the mean-field theory and studied finite-size systems with Monte Carlo method. We searched the ground state restricting ourselves to spin configurations with up to four-sublattice structures within the mean-field theory. To take into account larger sublattice structures, we studied larger finite-size systems and searched the minimum energy state with Monte Carlo method, gradually decreasing temperatures. Here we only discuss the phase (b), where the parameters are

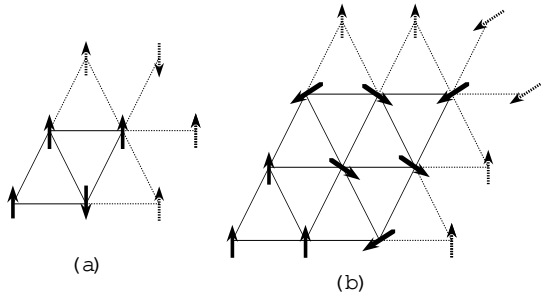


FIG. 1. Spin configuration of (a) *uuud* state with four sublattices and (b) a coplanar state with nine sublattices.

in $-8K < J < -8K/3$ and competitions of the two- and four-spin exchanges are strong.

If there is no magnetic field, ground states are highly degenerate for $-8K < J < -8K/3$. We list some ground states which we found:

1. A collinear state with a four-sublattice structure. Up spins are on three sublattices and down spin on the other (see Fig. 1a). We call this state as *uuud* state.
2. A coplanar state with nine sublattices, whose spin configuration is constructed from three kinds of spin vectors (see Fig. 1b).
3. Many other ground states can be made out of the *uuud* state by reversing all up spins to down on some parallel straight lines that consist of only up spins (see Fig. 2).

All these states have the minimum energy $E/N = -3K$. The *uuud* state has the largest magnetization $m/m_{\text{sat}} = 1/2$ among these states. The coplanar state shows $S^z = 0$ and the third series of ground states have a variety of magnetization between $-1/2 < m/m_{\text{sat}} < 1/2$. The number of degeneracy except for the $SO(3)$ symmetry is at least of order $2^{L/2}$ on the $L \times L$ triangular lattice, which comes from line degrees of freedom for spin flips. The number of the states in the $S^z = ML$ sector, where M is an integer in $-L/2 \leq M \leq L/2$, is at least $L/2 C_{(L-2M)/4}$ and thus the degeneracy is largest in the $S^z = 0$ sector. This degeneracy does not originate from the symmetry of the Hamiltonian and instead comes from frustration effects. We suspect that strong frustration makes density of states large near the lowest energy and hence non-trivial degeneracy appears in the ground states.

Another characteristic property also appears in excitations. For the ground states in group 3, a huge number of excitations have extremely low energy, which is very close to the ground state energy. Consider a stripe excitation which is shown on Fig. 3. On the i th line, rotate spins with angle θ and, on the $i-1$ th and $i+1$ th lines, rotate spins with angle $\theta/2$, where i th line contains only up spins. For small θ , expanding the excitation energy

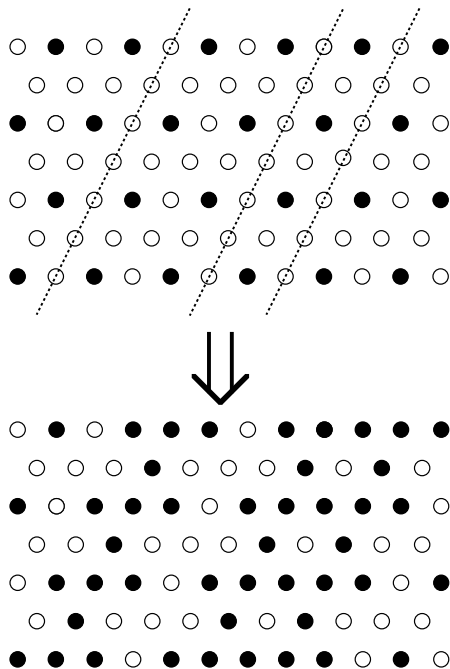


FIG. 2. Spin configuration of two kinds of ground states. Up (down) spins are denoted by white (black) circles. The upper configuration is that of the *uuud* state. The lower one is obtained by reversing the up spins to down on the dashed lines of the upper one.

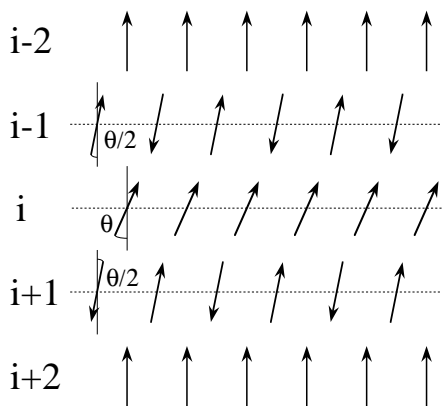


FIG. 3. A stripe excitation of the *uuud* state. Spins on the i th line are rotated with angle θ , and on the $i-1$ th and $i+1$ th lines with angle $\theta/2$.

with θ , one can find that, $\mathcal{O}(\theta^2)$ terms of the excitation energy vanish and the leading term starts from the order $\mathcal{O}(\theta^4)$, if all spins on both $i-2$ th and $i+2$ th lines direct upward. We note that line excitation energy usually depends on the angle θ in the quadratic form. The condition for the low excitations of this kind to appear is that all spins on three lines in next neighbors, *i.e.* on $i-2$ th, i th and $i+2$ th lines, are in the same direction with each other. We hence find that these low energy excitations exist for most of ground states in group 3 and there are a huge number of low-lying excitations of this kind.

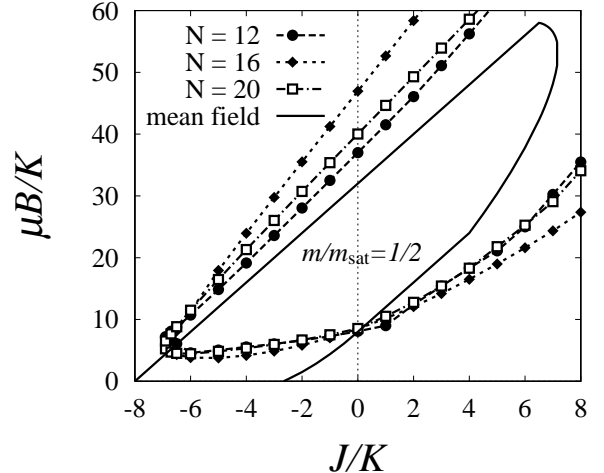


FIG. 4. Parameter dependence of phase boundaries of the $m/m_{\text{sat}} = 1/2$ state in the magnetization process at $T = 0$, where the $1/2$ -plateau appears in the region surrounded by data. The solid line denotes the result from the mean-field theory in the classical limit and other data with lines denote the results of the quantum model ($S = 1/2$) on finite-size systems.

By applying a weak magnetic field, this degeneracy quickly disappears. Since the *uuud* state has the largest magnetization among the degenerate states, the *uuud* state is stable under the magnetic field and it has the lowest energy. Figure 4 shows the parameter region where the *uuud* state becomes the ground state. The *uuud* state remains to be the ground state up to finite magnitude of the magnetic field, which means the magnetic susceptibility to be vanishing in this phase. This behavior occurs due to singularity of collinear states. Since all spin vectors in the *uuud* state are parallel to the magnetic field, spins can be rigid against the field. The *uuud* state hence makes a plateau at the half magnetization $m/m_{\text{sat}} = 1/2$ in the magnetization process (see Fig. 5). These results are obtained with the mean-field theory and also confirmed with Monte Carlo method. The *uuud* state can stably exist even at low but finite temperatures and it also shows a finite-temperature phase transition due to the breakdown of the translational symmetry. We will

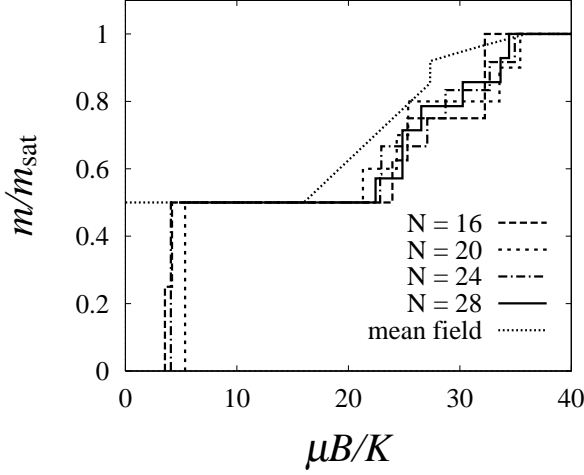


FIG. 5. Magnetization process at $T = 0$ for $J = -4$ and $K = 1$. The dotted line denotes the result from the mean-field theory in the classical limit¹⁹ and other lines denote the results of the quantum model ($S = 1/2$) on finite-size systems.

further discuss finite-temperature properties in section V.

III. QUANTUM ($S = 1/2$) MODEL WITH $B = 0$.

When there are various degenerate ground states in the classical limit, quantum effects play an essential role in forming the ground state of the quantum model. One possibility is that a new quantum ground state appears due to tunneling between the classical states. This mixture of states can occur between the degenerate ground states in the same S^z sector. This possibility was discussed as an origin of the disordered state which is observed in low-density solid ^3He films.^{19,5} Another possibility is that one of the degenerate ground states may be selected due to quantum effects.

To test these possibilities, we first examine the $uuud$ state, which is one of the classical ground states, with the spin-wave approximation. Using the Holstein-Primakoff transformation, we expand the Hamiltonian up to the quadratic form of bosons

$$\mathcal{H} = -3NK + \sum_k \mathbf{A}_k^\dagger \mathcal{D}_k \mathbf{A}_k \quad (3)$$

with $\mathbf{A}_k^\dagger = (a_k^\dagger, b_k^\dagger, c_k^\dagger, d_{-k})$ and

$$\mathcal{D}_k = \begin{pmatrix} -4J & B\mathbf{e}_2, 2\mathbf{e}_1 & B\mathbf{e}_2 - \mathbf{e}_1, 2\mathbf{e}_1 & C\mathbf{e}_1 \\ B\mathbf{e}_2, 2\mathbf{e}_1 & -4J & B\mathbf{e}_1, 2\mathbf{e}_2 & C\mathbf{e}_1 - \mathbf{e}_2 \\ B\mathbf{e}_2 - \mathbf{e}_1, 2\mathbf{e}_1 & B\mathbf{e}_1, 2\mathbf{e}_2 & -4J & C\mathbf{e}_2 \\ C\mathbf{e}_1 & C\mathbf{e}_1 - \mathbf{e}_2 & C\mathbf{e}_2 & 12(J + 8K) \end{pmatrix}, \quad (4)$$

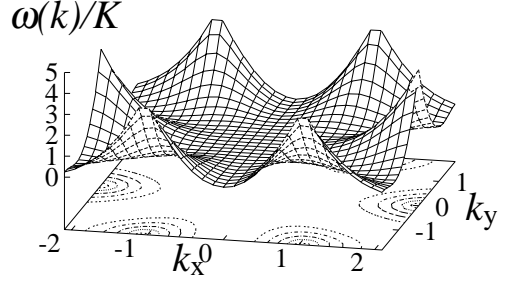


FIG. 6. The lowest mode of spin-wave spectrum on the $uuud$ ordered state. The contour is written on the bottom plane. Zero modes appear on the three lines, $k_x = 0$ and $k_y = \pm\sqrt{3}k_x/2$.

where a, b, c and d denote bosons for four sublattices and

$$\begin{aligned} B\mathbf{r}, \mathbf{r}' &= 4(J + 2K) \cos \mathbf{k} \cdot \mathbf{r} + 8K \cos \mathbf{k} \cdot (\mathbf{r} - \mathbf{r}'), \\ C\mathbf{r} &= 4(J + 8K) \cos \mathbf{k} \cdot \mathbf{r}. \end{aligned} \quad (5)$$

Numerically diagonalizing this Hamiltonian with Copla's method,²¹ we evaluate the excitation spectrum of spin waves.²² The spectrum has four branches of excitation modes in the 1st Brillouin zone of the four-sublattice structure. The lowest mode shows an ill behavior (see Fig. 6); it has flat modes along three lines in momentum space, $k_x = 0$ and $k_y = \pm\sqrt{3}k_x/2$, and furthermore the dispersion curves across the three lines have a form $|\mathbf{k} - \mathbf{k}_0|^6$. These modes correspond to the line excitations that we have shown for the classical model in Section II. This flat mode suggests that the $uuud$ state does not have spin stiffness. Higher-order terms of spin-wave expansions may destroy the $uuud$ state due to non-linear effects.

We also studied the ground state of finite-size systems with exact-diagonalization method. The systems with the size $N = 12, 16, 20, 24$ and 28 are treated. (See Appendix A for shapes of the finite-size clusters.) The results reveal that the ground state belongs to the $S = 0$ space and hence it is not the $uuud$ state for $-7K \leq J$, which almost covers the phase (b). Recent numerical study by Misguich et al.²³ also suggests that the ground state in the same parameter region is spin liquid with $S = 0$.

All the above results are consistent with each other and give a unique picture. The ground state belongs to the $S = 0$ space and the $uuud$ state has a little higher energy than the ground state due to quantum effects. The $uuud$ state thus disappears from the ground state in the quantum model. But it again becomes stable under the magnetic field. We will discuss this point in the next

section.

IV. QUANTUM ($S = 1/2$) MODEL UNDER THE MAGNETIC FIELD ($B > 0$).

To test the appearance of magnetization plateau at $m/m_{\text{sat}} = 1/2$ which we found in the classical limit, we investigate ground states of the quantum model (1) in finite-size systems under the magnetic field. We study finite-size ($N \leq 28$) systems with periodic-boundary conditions. Figure 5 shows the magnetization process of finite-size systems with $J = -4$ and $K = 1$. Though the magnetization increases stepwisely due to finite-size effects, there clearly exists a broad plateau at $m/m_{\text{sat}} = 1/2$ in every-size data. Width between the lower and upper critical fields of the plateau does not vanish, as the system size increases, and remains to be significantly large (see Fig. 7). This result strongly suggests that this magnetization plateau survives in the thermodynamic limit. To examine whether this $m/m_{\text{sat}} = 1/2$ state has the *uuud* long-range order, we consider the following *uuud* order parameter

$$\mathcal{O} = \frac{1}{2} \left(\sum_{i \in A} \sigma_i^z + \sum_{i \in B} \sigma_i^z + \sum_{i \in C} \sigma_i^z - \sum_{i \in D} \sigma_i^z \right) \quad (6)$$

and calculate long-range order

$$\langle \langle \mathcal{O}^2 \rangle - \langle \mathcal{O} \rangle^2 \rangle / N^2 \quad (7)$$

in the ground state of the $S_{\text{total}}^z = N/4$ space. Results are shown in Fig. 8, which clearly suggest that data are extrapolated to a finite value in the $N \rightarrow \infty$ limit for $J = -4K$. The extrapolated value is estimated as about 0.03 in the $N \rightarrow \infty$ limit. Long-range order of the *uuud* structure brings breakdown of translational symmetry in the thermodynamic limit. A careful estimation (see Appendix B) leads that, when the translational symmetry is spontaneous broken, the expectation value of spin on each sublattice is $\langle \sigma_i^z/2 \rangle = 0.45$ for $i \in A$, B - or C -sublattice, and $\langle \sigma_i^z/2 \rangle = -0.35$ for $i \in D$ -sublattice, respectively. The ground state in the $S_{\text{total}}^z = N/4$ space thus has a rigid *uuud* long-range order and deviation of the sublattice magnetization from the classical value is small. By the way, the total magnetization in the *uuud* ordered state does not change from the classical value $m/m_{\text{sat}} = 1/2$ by quantum effects. Note that the expectation values of spin satisfy $\sum_i \langle \sigma_i^z/2 \rangle / N = (3 \times 0.45 - 0.35)/4 = 1/4$. The spin-wave analysis also does not give any quantum correction to the total magnetization in the *uuud* state. The same feature was also observed in the magnetization plateau at $m/m_{\text{sat}} = 1/3$ for the antiferromagnet on the triangular lattice.²⁴ Recently Misguich et al.²³ also found a similar magnetic plateau at $m/m_{\text{sat}} = 1/2$ in a MSE model with two-, four- and six-spin exchanges. We believe that their plateau comes from the *uuud* ordered state and that the

four-spin exchange is the main cause for the plateau as well.

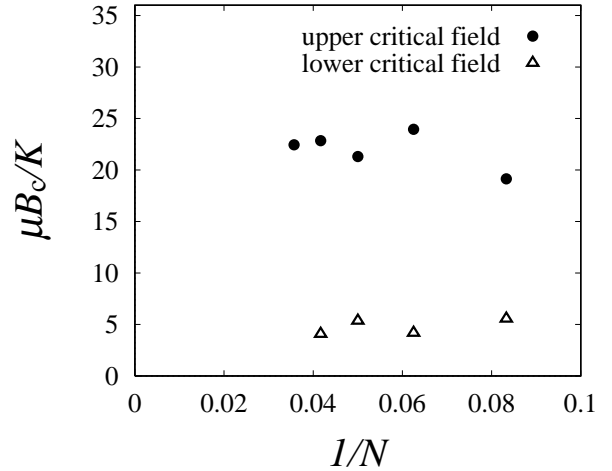


FIG. 7. Size dependence of the lower- and upper-critical fields of the magnetization plateau at $S_{\text{total}}^z = N/4$ for the model with $J = -4$ and $K = 1$.

Next, we study the excitations in the $S_{\text{total}}^z = N/4$ space. Figure 9 shows excitation energy of up to fourth excited state. Three low-lying excited states have almost same energy with the ground-state energy and they converge to the ground state as the system size is enlarged. Above them there is a large gap, which seems not to vanish in the $N \rightarrow \infty$ limit. Thus four states exist around the lowest level and are clearly separated from other excited states. The number of low-lying levels, four, is equal to that of the degenerate *uuud* states, which comes from translation of sublattices. Furthermore, the four low-lying states have the same translation group as the following schematic states, respectively,

$$\begin{aligned} |1\rangle &= (1 + \mathcal{R}_1 + \mathcal{R}_2 + \mathcal{R}_1 \mathcal{R}_2) |\uparrow\uparrow\downarrow\downarrow\rangle, \\ |2\rangle &= (1 + \mathcal{R}_1 - \mathcal{R}_2 - \mathcal{R}_1 \mathcal{R}_2) |\uparrow\uparrow\downarrow\downarrow\rangle, \\ |3\rangle &= (1 - \mathcal{R}_1 + \mathcal{R}_2 - \mathcal{R}_1 \mathcal{R}_2) |\uparrow\uparrow\downarrow\downarrow\rangle, \\ |4\rangle &= (1 - \mathcal{R}_1 - \mathcal{R}_2 + \mathcal{R}_1 \mathcal{R}_2) |\uparrow\uparrow\downarrow\downarrow\rangle, \end{aligned} \quad (8)$$

where $|\uparrow\uparrow\downarrow\downarrow\rangle$ denotes one of the *uuud* states, $\otimes_{i \in A, B, C} |\uparrow\rangle_i \otimes_{j \in D} |\downarrow\rangle_j$, and \mathcal{R}_i ($i = 1, 2$) mean translation of sites by unit vectors \mathbf{e}_i . We hence believe that these four levels form four ground states which have *uuud* order in the thermodynamic limit and translational invariance is spontaneously broken in the ground states. This argument leads to a conclusion that the fifth low-lying state corresponds to the lowest excitation in the thermodynamic limit and hence the spin excitation spectrum has a finite gap in the same S_{total}^z sector.

The appearance of the magnetization plateau and the excitation gap may be understood by introducing a particle picture into the spin model.²⁵ If we regard the down

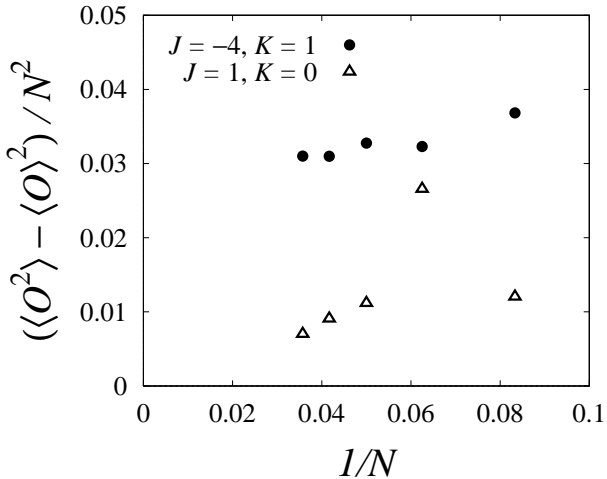


FIG. 8. Size dependence of long-range order of the *uuud* structure, $\langle\langle O^2 \rangle - \langle O \rangle^2\rangle/N^2$, in the ground state of the $S_{\text{total}}^z = N/4$ space. Black circles denote data for the model with $J = -4$ and $K = 1$. Data for the Heisenberg antiferromagnet ($J = 1$, $K = 0$) are also shown with triangle symbols for a comparison.

spins as particles moving in background of up spins and the magnetic field μB as minus of the chemical potential of the particle, we can recognize the *uuud* order as a charge-density wave (CDW). Note that this density wave can be ordered by repulsion between particles on nearest- or next-nearest-neighbor pairs of sites and this repulsion originates from the four-spin exchange interaction. In CDW, particles are insulating and charge-density excitations have a finite gap. Then the compressibility is vanishing. Through the mapping, these features correspond to the finite excitation gap and the magnetization plateau of the spin model. This scenario in the particle picture gives an explanation for the plateau from the particle limit ($S = 1/2$).²⁶ As we mentioned in section II, the appearance of the plateau in the $S \rightarrow \infty$ limit originates from the rigidity of the collinear state. If the scenario in the particle picture is valid, the mechanism for appearance of the plateau is understood both from the classical limit ($S \rightarrow \infty$) and the particle limit ($S = 1/2$). Note that, in both cases, the *uuud* order is the key property for the appearance of the magnetization plateau.

The $1/2$ -plateau appears for a wide parameter region. In Fig. 4, we show the phase boundary of the parameter region of the plateau. Except for weak magnetic field cases, the region of the $m/m_{\text{sat}} = 1/2$ phase becomes wider in comparison with the classical model. Quantum effects thus stabilize the plateau and enhance its appearance.

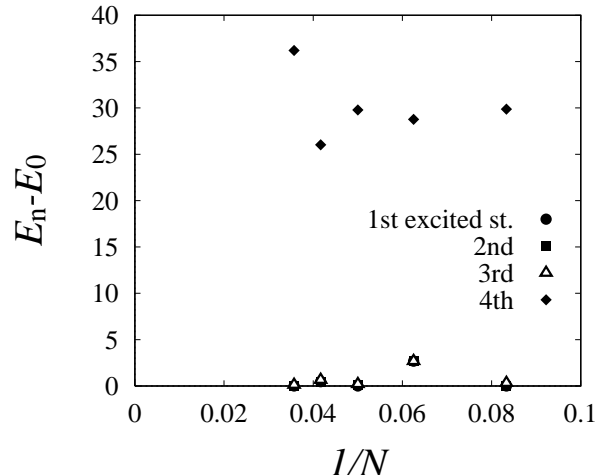


FIG. 9. Size dependence of excitation energy of four low-lying excited states in the $S_{\text{total}}^z = N/4$ space for the model with $J = -4$ and $K = 1$. The symbol for the third excited state almost overlaps those for the first and second states.

V. THERMAL EFFECTS

It is also important to discuss thermal effects to the magnetization plateau for a comparison with experiments at finite temperatures. We study the finite-temperature properties in the classical limit using Monte Carlo simulations with the Metropolis algorithm. If a spin flip is rejected, we randomly rotate the spin about the local molecular field. We construct finite-size systems with a unit cluster which has 12 sites. The system size is $N = 12L^2$ with $L = 4, 6, 8, 12, 16$ with a periodic-boundary condition. After discarding initial 30000–50000 Monte Carlo steps per spin (MCS) for equilibration, subsequent 3×10^5 – 5×10^5 MCS are used to calculate the average.

Fortunately, this magnetization plateau survives even at low temperatures. This can be easily shown by Monte Carlo simulations of the classical model at finite temperatures (see Fig. 10). Since the number of ground states is four under the magnetic field and the system is in two dimensions, the breakdown of the translational symmetry can occur even at a finite temperature, and the state below the critical temperature can have a *uuud* long-range order. Magnetization of the *uuud* ordered state is close to $m/m_{\text{sat}} = 1/2$ at low temperatures and it makes a plateau (or a shoulder) near the half of the saturated magnetization. Misguich et al.²³ also demonstrated the stability of the plateau at finite low temperatures in the quantum MSE model on a finite-size ($N = 24$) lattice. Similarly, magnetization plateau at $m/m_{\text{sat}} = 1/3$ was successfully observed at finite temperatures in the measurements of C_6Eu ²⁷ and CsCuCl_3 ,²⁸ and in Monte Carlo

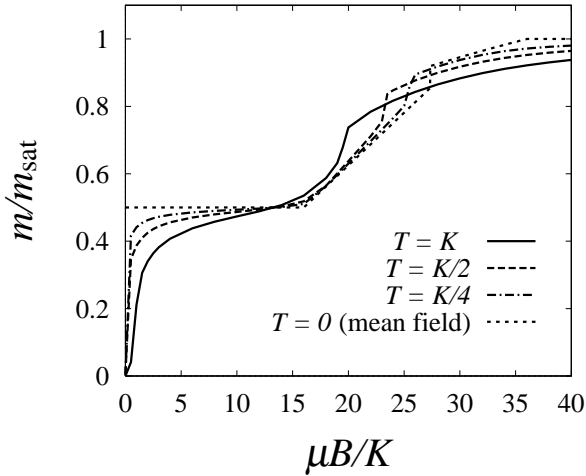


FIG. 10. Magnetization process of the classical model with $J = -4$ and $K = 1$ at finite temperatures $T/K = 0.25$, 0.5 and 1.0 . The magnetization process at zero temperature, which we obtained with the mean-field theory,¹⁹ is also shown for a comparison.

simulations of the Heisenberg antiferromagnet on the triangular lattice.²⁹

Another favorable property of the *uuud* order is that it accompanies a phase transition at a finite temperature. We studied the classical model under a magnetic field which realizes the *uuud* ground state. Monte Carlo simulations show a sharp divergence in the specific-heat data (Fig. 11) and formation of the *uuud* order below the critical temperature. Near the critical temperature, the magnetization curve is still rounded and smooth. As lowering the temperature, the slope of the curve decreases and becomes flat near $m/m_{\text{sat}} = 1/2$. The critical temperature is estimated as $T_c = 1.9K$ for the model with $J = -4K(< 0)$ and $\mu B = 10K$. For a weak magnetic field $\mu B = 5K$, the estimate of T_c is about $1.7K$. These values can change due to quantum effects in the $S = 1/2$ model. From the degeneracy of the ground state, the phase transition is expected to be of second order and to belong to the 4-state Potts universality class. The finite-size scaling analysis, however, shows that critical exponent α is much larger than the expected value $\alpha = 2/3$ ³⁰ for the 4-state Potts model. Moreover distribution of energy histogram in Monte Carlo simulations has two peaks at the critical temperature, which suggests that the phase transition is of first order. A similar deviation of the universality was also found in the phase transition of chiral symmetry breaking in the model (1) for strong K .^{20,31} These deviations may come from frustration effects, or singularity of four-body interactions. Critical properties of these phase transitions will be discussed further in a forthcoming paper.

The discrete symmetry of the *uuud* order in a mag-

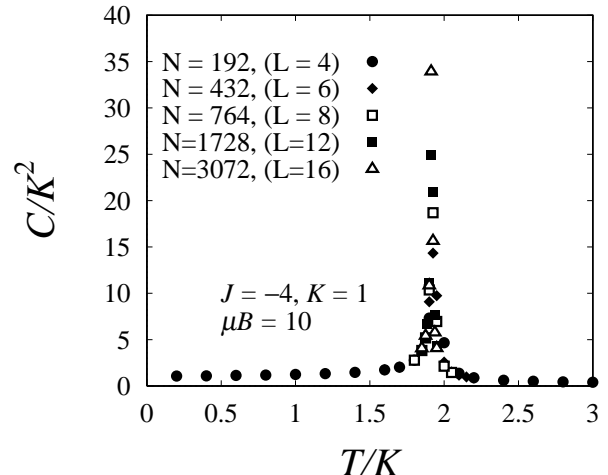


FIG. 11. Temperature dependence of the specific heat of the classical model with $J = -4$, $K = 1$ and $\mu B = 10$. Monte Carlo simulations were done on triangular lattices with finite size $N = 12L^2$.

netic field accompanies two favorable properties that the magnetization plateau stably exists at low but finite temperatures and a sharp phase transition occurs at a finite temperature. We expect that these properties make the experimental observation of the magnetization plateau possible.

VI. SUMMARY AND DISCUSSION

In this paper, we examined the appearance of the magnetization plateau at $m/m_{\text{sat}} = 1/2$ in a 2D MSE model on the triangular lattice, which we predicted in our previous work. This plateau appears when the two- and four-spin exchange interactions compete strongly, which may be realized in 2D low-density solid ^3He , and if the five- and six-exchanges are not too strong. The four-spin exchange is important and relevant to make the plateau at $m/m_{\text{sat}} = 1/2$. Experimental observation of this plateau in the magnetization process of the solid ^3He films will confirm that the four-spin exchange are strong and important. The plateau survives even at low but finite temperatures and it accompanies a phase transition at a finite temperature. In our model with $J = -4K(< 0)$, the lower critical field of the plateau is estimated about $4K/\mu$. Setting the parameter as $K = 1.5(\text{mK})$ and $\mu = 2.13\mu_N$, where $\mu_N = 0.366(\text{mK/T})$, we estimate the lower critical field as $B_c \simeq 7[T]$. Since this magnitude of the field is accessible with the present experimental equipments, we expect experimental verification of the magnetization process to be possible in 2D low-density solid ^3He .

ACKNOWLEDGMENTS

The authors would like to thank Hiroshi Fukuyama and Hikaru Kawamura for stimulating discussions and comments. One of the authors (T.M.) acknowledges Keisuke Totsuka for useful discussions and K.K. acknowledges J. Saunders, C. Lhuillier and G. Misguich for useful discussions. This work was supported by Grant-in-Aid Nos. 09440130 and 10203202 from the Ministry of Education, Science and Culture of Japan. The numerical calculations were done on Facom VPP500 at the ISSP of the University of Tokyo and DEC Alpha 500 personal workstation at the Institute of Physics of the University of Tsukuba. K.K. also acknowledges the EPSRC Visiting Fellowship Grant GR/L 90804 and the kind hospitality at the Department of Mathematics, Imperial College, London, where a part of this work was accomplished.

APPENDIX A: CLUSTERS USED IN FINITE-SIZE STUDIES.

In the numerical study of the $S = 1/2$ model on finite-size systems, we used finite-size clusters with the periodic boundary condition which matches the four-sublattice structure. Clusters are set on the triangular lattice as shown in Fig. 12.

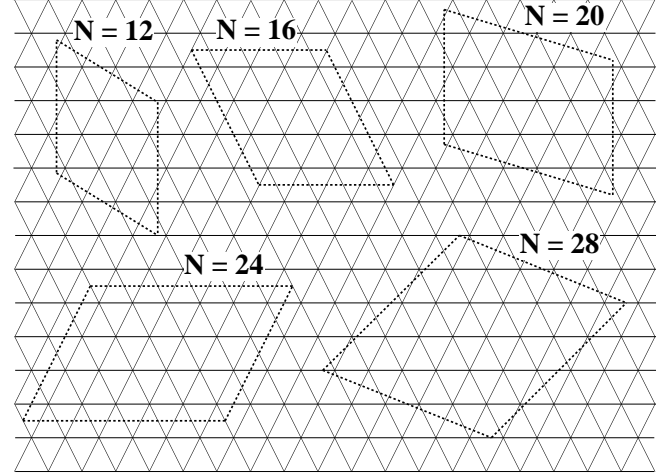


FIG. 12. Finite-size clusters which we used in the exact diagonalization study.

APPENDIX B: EVALUATION OF EXPECTATION VALUES OF THE SUBLATTICE MAGNETIZATION.

Estimation of the sublattice magnetization from the long-range order (7) needs a careful consideration about symmetry breaking. In the thermodynamic limit, translational symmetry is spontaneously broken in a pure natural ground state with *uuud* order. But the ground states of finite-size systems become mixed symmetric ones because of finite-size effects.

Here we write the mixed symmetric ground state in the $S_{\text{total}}^z = N/4$ space as $|\phi\rangle$. We also consider a state $|\psi_1\rangle$ in which translational symmetry is broken and whose thermodynamic limit is the natural pure ground state. By the space translation of the state, $|\psi_1\rangle$ relates to other three *uuud* ordered states in the form

$$|\psi_2\rangle = \mathcal{R}_1|\psi_1\rangle, \quad |\psi_3\rangle = \mathcal{R}_2|\psi_1\rangle, \quad |\psi_4\rangle = \mathcal{R}_1\mathcal{R}_2|\psi_1\rangle, \quad (B1)$$

where \mathcal{R}_1 (\mathcal{R}_2) denotes spatial translation by e_1 (e_2). In the mixed state, there is translational invariance,

$$\langle\phi|S_i^z|\phi\rangle = \frac{1}{4} \quad \text{for any site } i. \quad (B2)$$

On the other hand, in the *uuud* ordered state $|\psi_1\rangle$, the translational symmetry is broken,

$$\langle\psi_1|S_i^z|\psi_1\rangle = m_1 \quad \text{for } i \in A, B \text{ or } C, \quad (\text{B3})$$

$$\langle\psi_1|S_i^z|\psi_1\rangle = m_2 \quad \text{for } i \in D, \quad (\text{B4})$$

where $m_1 \neq m_2$. Since the total magnetization is $N/4$, the sublattice magnetization m_1 and m_2 satisfy

$$\frac{3}{4}m_1 + \frac{1}{4}m_2 = \frac{1}{4}. \quad (\text{B5})$$

It is expected that the symmetric mixed state can be decomposed into the pure states in the thermodynamic limit in the form $|\phi\rangle = (|\psi_1\rangle + e^{i\theta}|\psi_2\rangle + e^{i\psi}|\psi_3\rangle + e^{i\phi}|\psi_4\rangle)/2$, where θ, ψ and ϕ denote arbitrary real numbers. The following relation hence holds in the large N limit:

$$\begin{aligned} \frac{1}{N^2}\langle\phi|\mathcal{O}^2|\phi\rangle &= \frac{1}{4N^2}(\langle\psi_1|\mathcal{O}^2|\psi_1\rangle \\ &\quad + \langle\psi_2|\mathcal{O}^2|\psi_2\rangle + \langle\psi_3|\mathcal{O}^2|\psi_3\rangle + \langle\psi_4|\mathcal{O}^2|\psi_4\rangle). \end{aligned} \quad (\text{B6})$$

From the numerical calculations in section IV, we have

$$\lim_{N \rightarrow \infty} \frac{1}{N^2}\langle\phi|\mathcal{O}^2|\phi\rangle = 0.03 + \left(\frac{1}{8}\right)^2. \quad (\text{B7})$$

For the pure state, the clustering property of the state leads

$$\begin{aligned} \lim_{N \rightarrow \infty} \frac{1}{N^2}\langle\psi_1|\mathcal{O}^2|\psi_1\rangle &= \left(\lim_{N \rightarrow \infty} \frac{1}{N}\langle\psi_1|\mathcal{O}|\psi_1\rangle\right)^2 \\ &= \left\{\frac{1}{4}(3m_1 - m_2)\right\}^2 \end{aligned} \quad (\text{B8})$$

and

$$\begin{aligned} \lim_{N \rightarrow \infty} \frac{1}{N^2}\langle\psi_2|\mathcal{O}^2|\psi_2\rangle &= \left(\lim_{N \rightarrow \infty} \frac{1}{N}\langle\psi_2|\mathcal{O}|\psi_2\rangle\right)^2 \\ &= \left\{\frac{1}{4}(m_1 + m_2)\right\}^2. \end{aligned} \quad (\text{B9})$$

In the same way,

$$\begin{aligned} \lim_{N \rightarrow \infty} \frac{1}{N^2}\langle\psi_3|\mathcal{O}^2|\psi_3\rangle &= \lim_{N \rightarrow \infty} \frac{1}{N^2}\langle\psi_4|\mathcal{O}^2|\psi_4\rangle \\ &= \left\{\frac{1}{4}(m_1 + m_2)\right\}^2. \end{aligned} \quad (\text{B10})$$

Inserting these relations into eq. (B6) and using eq. (B5), we have

$$48m_1^2 - 24m_1 + 1.08 = 0 \quad (\text{B11})$$

and then we obtain two solutions $(m_1, m_2) = (0.45, -0.35)$ and $(0.005, 0.985)$. From the constraints $|m_1| \leq 0.5$ and $|m_2| \leq 0.5$, we conclude that the former one is the physical solution.

¹ P. A. M. Dirac, *The Principles of Quantum Mechanics* (Clarendon, Oxford, 1947).

² D. J. Thouless, Proc. Phys. Soc. (London) **86**, 893 (1965).

³ M. Siqueira, J. Nyéki, B. Cowan and J. Saunders, Phys. Rev. Lett. **76**, 1884 (1996).

⁴ M. Roger, C. Bäuerle, Yu. M. Bunkov, A.-S. Chen, and H. Godfrin, Phys. Rev. Lett. **80**, 1308 (1998).

⁵ K. Ishida, M. Morishita, K. Yawata and H. Fukuyama, Phys. Rev. Lett. **79**, 3451 (1997).

⁶ J. M. Delrieu, M. Roger, and J. H. Hetherington, J. Low Temp. Phys. **40**, 71 (1980).

⁷ M. Roger, Phys. Rev. B **30**, 6432 (1984).

⁸ B. Bernu, D. Ceperley and C. Lhuillier, J. Low Temp. Phys. **89**, 589 (1992).

⁹ M. Katano and D. Hirashima, private communication; M. Katano, Master Thesis, (University of Tsukuba, 1998).

¹⁰ G. Misguich, B. Bernu, C. Lhuillier, and D. Ceperley, private communication.

¹¹ H. Franco, R. Rapp and H. Godfrin, Phys. Rev. Lett. **57**, 1161 (1986); H. Godfrin, R. Ruel and D. Osheroff, Phys. Rev. Lett. **60**, 305 (1988); H. Godfrin, R. E. Rapp and H. J. Lauter, Physica B **169**, 177 (1991).

¹² P. Schiffer, M. T. O'Keefe, D. D. Osheroff and H. Fukuyama, Phys. Rev. Lett. **71**, 1403 (1993); J. Low Temp. Phys. **94**, 489 (1994).

¹³ M. Siqueira, C.P. Lusher, B.P. Cowan and J. Saunders, Phys. Rev. Lett. **71**, 1407 (1993).

¹⁴ M. Morishita, K. Ishida, K. Yawata and H. Fukuyama, Czech. J. Phys. Suppl. S1 **46**, 409 (1996).

¹⁵ M. Siqueira, J. Nyéki, B. Cowan and J. Saunders, Czech. J. Phys. Suppl. S6 **46**, 3033 (1996); Phys. Rev. Lett. **78**, 2600 (1997).

¹⁶ D. S. Greywall and P. A. Busch, Phys. Rev. Lett. **62**, 1868 (1989); D. S. Greywall, Phys. Rev. B **41**, 1842 (1990).

¹⁷ M. Roger, J.H. Hetherington and J.M. Delrieu, Rev. Mod. Phys. **55**, 1 (1983).

¹⁸ M. Roger, Phys. Rev. Lett. **64**, 297 (1990).

¹⁹ K. Kubo and T. Momoi, Z. Phys. B. **103**, 485 (1997).

²⁰ T. Momoi, K. Kubo, and K. Niki, Phys. Rev. Lett. **79**, 2081 (1997).

²¹ J. H. P. Copla, Physica **93A**, 327 (1978).

²² K. Kubo, K. Niki and T. Momoi, in preparation.

²³ G. Misguich, B. Bernu, C. Lhuillier, and C. Waldtmann, Phys. Rev. Lett. **81**, 1098 (1998).

²⁴ A. E. Jacobs, T. Nikuni and H. Shiba, J. Phys. Soc. Jpn. **62**, 4066 (1993).

²⁵ A particle picture succeeded to explain the appearance of the magnetization plateau in the one-dimensional $S = 1/2$ dimerized Heisenberg antiferromagnets and $S = 1$ bond alternating ones. See K. Totsuka, Phys. Rev. B **57**, 3454 (1998).

²⁶ K. Totsuka, private communication.

²⁷ H. Suematsu, K. Ohmatsu, K. Sugiyama, T. Sakakibara, M. Motokawa and M. Date, Solid State Commun. **40**, 241 (1981); T. Sakakibara, K. Sugiyama, M. Date and H. Suematsu, Synthetic Metals, **6**, 165 (1983).

²⁸ H. Nojiri, Y. Tokunaga and M. Motokawa, J. Phys. (Paris) **49** Suppl. C8, 1459 (1988).

²⁹ H. Kawamura and S. Miyashita, J. Phys. Soc. Jpn. **54**, 4530 (1985).

³⁰ F.Y. Wu, Rev. Mod. Phys. **54** (1982) 235.

³¹ Critical exponents were estimated as $\alpha = 0.62 \pm 0.05$ and $\beta = 0.090 \pm 0.008$ from finite-size scaling analysis. However there remains another possibility that the phase transition is of first order and critical exponents are wrongly estimated due to smallness of system size. Indeed, distribution of energy histogram for systems with large size ($N \geq 3072$) have two peaks which are very close to each other near the critical temperature.